

# Unsteady Pressure and Structural Response Measurements on an Elastic Supercritical Wing

Clinton V. Eckstrom,\* David A. Seidel,† and Maynard C. Sandford\*  
*NASA Langley Research Center, Hampton, Virginia 23665-5225*

Results are presented that define unsteady flow conditions associated with high dynamic response experienced on a high-aspect-ratio elastic supercritical wing at transonic test conditions while being tested in the NASA Langley Transonic Dynamics Tunnel. The supercritical wing, designed for a cruise Mach number of 0.80, experienced the high dynamic response in the Mach number range from 0.90 to 0.94, with the maximum response occurring at a Mach number of approximately 0.92. At the maximum wing response condition the forcing function appears to be the oscillatory chordwise movement of strong shocks located on both the wing upper and lower surfaces in conjunction with the flow separating and reattaching in the trailing-edge region.

## Nomenclature

|         |  |
|---------|--|
| $C_p$   | = pressure coefficient                                 |
| $C_p^*$ | = critical pressure coefficient, two-dimensional value |
| $G$     | = acceleration/gravitational constant                  |
| $M$     | = freestream Mach number                               |
| $q$     | = freestream dynamic pressure, psf                     |
| $x/c$   | = fraction of local chord                              |
| $\eta$  | = fraction of semispan                                 |

## Introduction

THE elastic supercritical wing used in the present test is the full-scale right semispan of the second Aeroelastic Research Wing (ARW-2). This research wing was designed to be flown on a drone flight aircraft for the investigation of active control systems for maneuver load alleviation, gust load alleviation, and flutter suppression.<sup>1</sup> The flight wing structural design was based on an iterative procedure that took into account the load and stiffness reduction benefits provided by the active control systems. This integrated design process resulted in a wing with more flexibility than otherwise would have occurred. A delay in the planned drone flight-test program provided the opportunity to use the instrumented flight wing as a flexible model for testing in the NASA Langley Transonic Dynamics Tunnel (TDT), as part of a continuing series of tests for measurement of unsteady transonic aerodynamic characteristics on various wing planforms and airfoil shapes.<sup>2</sup> In preparation for flight tests of the flexible wing, there were wind tunnel tests of a structurally stiff 0.237-scale model of the flight wing and drone fuselage.<sup>3,4</sup> These scale-model tests identified that the drag-divergence Mach number for this supercritical wing configuration occurs in the Mach number range 0.81 to 0.83. Drag-divergence is an indicator of the onset of the breakdown in attached flow conditions.

During the initial wind tunnel test of this elastic wing,<sup>5</sup> a region of high dynamic response characterized by wing first

bending motion was unexpectedly encountered near  $M=0.90$ . Analysis of wing response data using a subcritical response technique appeared to predict an instability boundary at an almost constant Mach number of 0.90 for all test dynamic pressures. Consequently, further testing was limited to  $M=0.88$  or less to prevent possible damage to the wing which was still considered to be a flight article. Although a change in flow characteristics at Mach numbers higher than drag-divergence was expected, the occurrence of large amplitude wing response motion and the resulting prediction of an instability boundary were not anticipated.

As a result of continued interest in the large amplitude wing response experienced during the first tunnel test and the subsequent cancellation of the flight-test program, a second tunnel test was conducted, without a Mach number limitation, to specifically investigate the region of large wing response. No instability boundary was found during the second test, but rather a narrow Mach number region through which the wing experiences high dynamic response.<sup>6</sup> The response, which increased in magnitude as the test dynamic pressure was increased, is centered near a Mach number of 0.92.

The goal for the second tunnel test was not only to explore fully the region of large wing response and determine if an instability boundary existed, but also to define the unsteady flow conditions forcing the response. The flexible ARW-2 wing was instrumented for the measurement of unsteady pressures on the outboard portion of the right semispan in preparation for the drone flight-test program. Measurement requirements for the first wind tunnel test resulted in the data being recorded for discrete test points to provide mean pressure values for static test conditions and transfer function magnitude and phase information for control surface oscillation tests. In order to provide better information on wing surface flow conditions, the data acquisition procedure was modified for the second test so that continuous wing surface-pressure time-history measurements were recorded. A summary of initial results from the second tunnel test were reported in Ref. 6. The conclusion that the driving mechanism appears to be related to chordwise shock movement in conjunction with flow separation and reattachment on both the wing upper and lower surfaces resulted from evaluation of the measured surface pressure time histories.

This paper presents sample results from an ongoing evaluation of the measured wing motions and wing surface pressure time histories. Sample pressure time histories and chordwise pressure distributions, showing the range of pressure measurement variation at each measurement location, are presented to show the degree of flow unsteadiness through the transonic speed range where the high dynamic response was en-

Presented as Paper 88-2277 at the AIAA/ASME/ASCE/AHS 29th Structures, Structural Dynamics, and Materials Conference, Williamsburg, VA, April 18-20, 1988; received June 4, 1988; revision received June 15, 1989. Copyright © 1989 American Institute of Aeronautics and Astronautics, Inc. No copyright is asserted in the United States under Title 17, U.S. Code. The U.S. Government has a royalty-free license to exercise all rights under the copyright claimed herein for Governmental purposes. All other rights are reserved by the copyright owner.

\*Aerospace Engineer, Configuration Aeroelasticity Branch, Structural Dynamics Division. Member AIAA.

†Aerospace Engineer, Unsteady Aerodynamics Branch, Structural Dynamics Division. Member AIAA.

countered. The effects of changes in test dynamic pressure and model angle of attack on mean value pressure distributions are also presented.

### Model

The right semispan of the full-scale wing used as the test model is shown mounted on the TDT test-section sidewall in Fig. 1. The supercritical wing model has a semispan length of 9.5 ft, an aspect ratio of 10.3, and a leading-edge sweep angle of 28.8 deg. The half-body fuselage has ogive nose and tail sections but is of cylindrical shape, with a diameter of 25 in. in the region of the wing mounting. Wing planform and dimensional data are presented in Fig. 2. The wing frequency response characteristics measured in still air are shown in Fig. 3. The four nodal frequencies noted in Fig. 3 are for the wing first bending, wing second bending, fore and aft in plane, and wing first torsion modes, respectively.

### Instrumentation

Locations for the wing surface-pressure orifices and the accelerometers are presented in the planform layout of Fig. 2. The wing surface pressures were measured using a separate electronically scanned pressure (ESP) measurement system<sup>7</sup> for each orifice row. Each ESP module contained 32 pressure transducers, all of which had a common reference pressure port. For this test setup, the reference pressure was the tunnel static pressure. The wing surface orifices were connected to the pressure transducers by matched metal and plastic tubes having an inner diameter of 0.040 in. and a length of 18 in. There were 16 orifices on both the upper and lower surfaces of the inboard orifice row and 15 orifices each on the upper and lower surfaces of the other five orifice rows, for a total of 182 wing surface pressure measurements. An additional eight in situ pressure transducers were located side by side with some of the fifth row orifices for calibration purposes.



Fig. 1 Wing mounted in TDT test section.

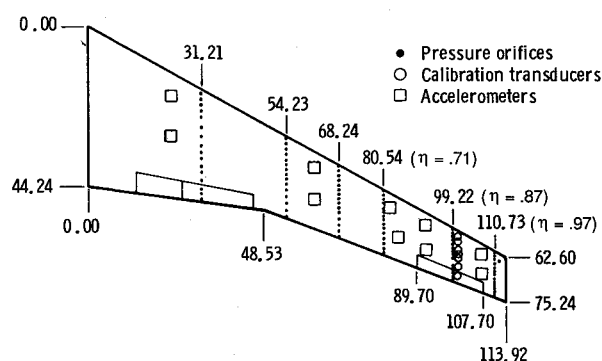


Fig. 2 Wing planform and instrumentation locations (in inches).

Wing vertical response motion was measured using 10 accelerometers located along the wing front and rear spars with the distribution shown in Fig. 2. Although not shown in Fig. 2, the wing was also equipped with several strain-gage bridges calibrated for the measurement of shear, bending moment, and torsion loads.<sup>8</sup>

### Data Acquisition

Data from the three inboard rows of orifices were acquired at a rate of 31.25 samples/s while for the three outboard rows of orifices the data were acquired at a rate of 250 samples/s. Data from the outboard six accelerometers and for four strain-gage bridges were also taken at a rate of 250 samples/s. The four strain-gage bridges used were located two each on the front and rear spars near the wing root. Data from the three outboard orifice rows, the wing tip leading-edge accelerometer, and the wing root rear spar bending moment strain-gage bridge were used for the analysis results presented herein.

### Wind Tunnel

The model was tested in the NASA Langley Research Center Transonic Dynamics Tunnel (TDT), which is a closed-circuit continuous-flow tunnel with a 16-ft square test section with slots in all four walls. Mach number and dynamic pressure can be varied simultaneously, or independently, with either air or Freon as the test medium. Freon was used for the testing reported herein.

### Test Results and Discussion

The supercritical wing model was tested by making runs at three different dynamic pressure ( $q$ ) levels as a function of Mach number as shown by the data in Fig. 4. The tunnel was operated by setting a total pressure and then increasing the motor fan speed until the desired test condition was reached. As a result the test dynamic pressure increased slightly with Mach number during each run, as shown in Fig. 4. The dynamic pressure at  $M=0.92$  for the low- $q$ , medium- $q$ , and high- $q$  test conditions were 78, 152, and 318 psf, respectively. Also shown in Fig. 4 is the region where high dynamic wing

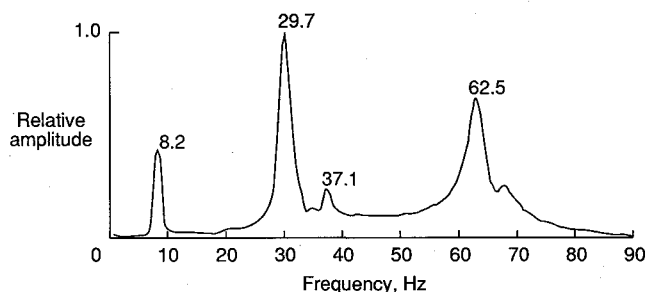


Fig. 3 Wing frequency response characteristics measured in still air.

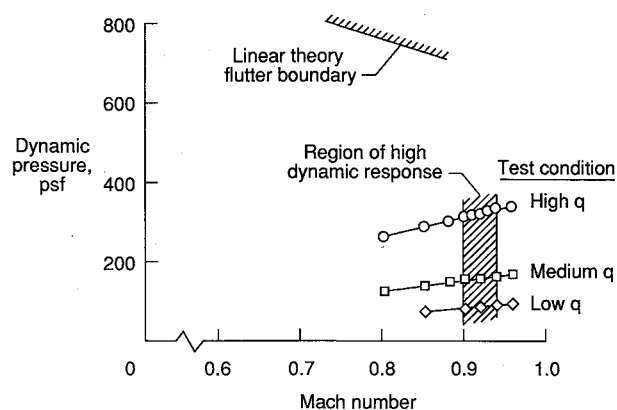


Fig. 4 Test conditions.

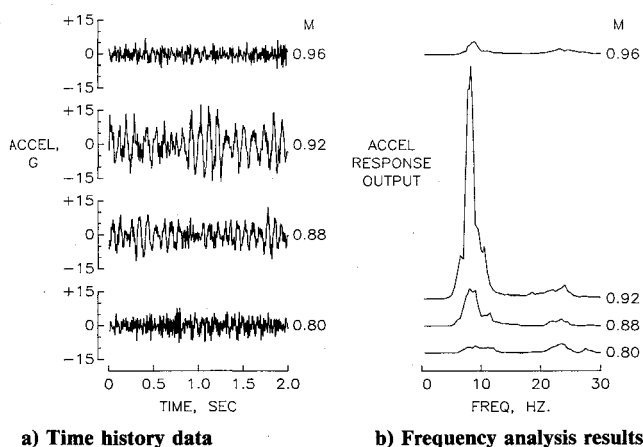


Fig. 5 Wing response measurements for high- $q$  test condition.

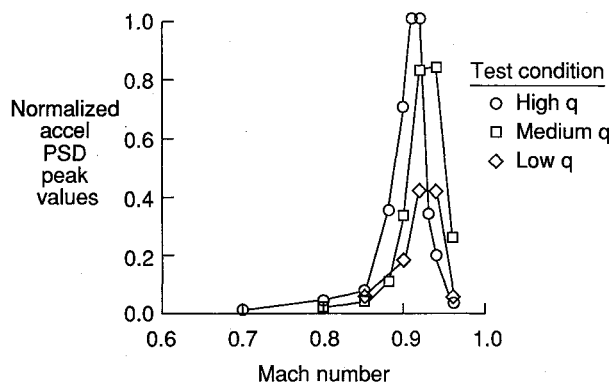


Fig. 6 Accelerometer PSD peak responses.

motion response was observed and measured, as well as the predicted linear theory flutter boundary, which is located at a much higher dynamic pressure level than where the wing was tested.

At the low- $q$  test conditions, all data were acquired at 0 deg angle of attack. For the medium- $q$  test conditions the angle of attack was varied from  $-2$  to  $+2$  deg in 1-deg increments. For the high- $q$  test condition, the primary angle of attack was 0 deg, although a few test points were obtained at  $\pm 1$  deg angle of attack. Unless otherwise stated, the data presented are for 0 deg angle of attack.

### Wing Response Measurements

Accelerometer measurement time histories and results from real-time response analysis of the accelerometer signals are presented in Fig. 5 for the high- $q$  test condition to illustrate the rapid growth and then the equally rapid decay of wing response as Mach number was increased from 0.80 to 0.96. The test Mach numbers selected are representative of conditions before any significant wing motion occurred ( $M=0.80$ ), during buildup of wing motion ( $M=0.88$ ), near maximum wing response ( $M=0.92$ ), and after wing motion had subsided ( $M=0.96$ ). The response measurements show that the frequencies for the large wing responses were in the 8–10 Hz range, which indicates that wing first bending mode type motion was occurring.

During post test analysis, a 10.24 s record of data was analyzed to define a power spectral density (PSD) curve for each of the test conditions shown previously in Fig. 4. For each test condition the maximum accelerometer PSD value in the 8–10 Hz frequency range was established. These maximum or peak PSD values are presented in Fig. 6, as a function of Mach number for each of the three dynamic pressure test conditions to show the narrow Mach number range through which the wing experienced the high dynamic response. The results pre-

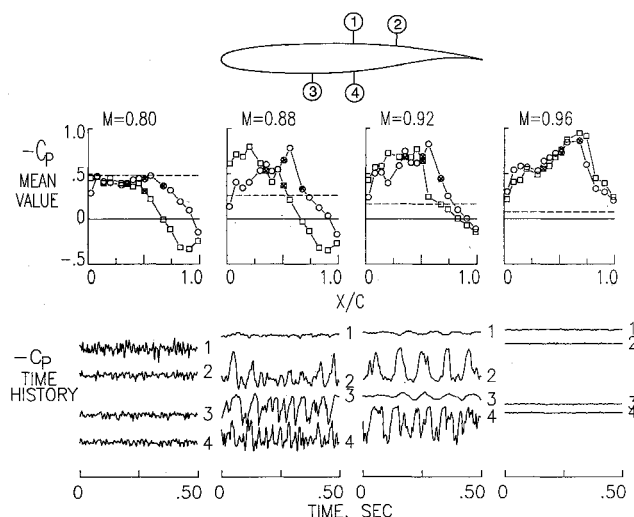


Fig. 7 Mean-value chordwise pressure distributions and sample pressure measurement time histories (high- $q$  test condition,  $q = 0.87$ ).

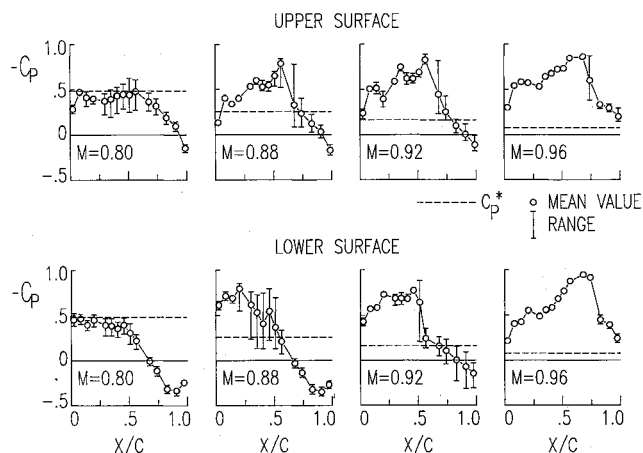


Fig. 8 Chordwise pressure distribution mean values and measurement ranges for representative Mach numbers (high- $q$  test condition,  $q = 0.87$ ).

sented in Fig. 6 also show that the peak values increased in magnitude as the test dynamic pressure increased and that the maximum wing response occurred near  $M=0.92$  for all three dynamic pressure test conditions.

### Presentation of Surface Pressure Measurements

Wing surface-pressure measurements are most often presented as chordwise distributions of time averaged or mean values of pressure coefficients for specific test conditions. Mean value results may be used because of instrumentation limitations that preclude getting valid time-history measurements, or mean value pressures may be used simply as a way to present a large number of results in a compact and efficient manner. Unfortunately, such a presentation method can mask time varying or unsteady flow conditions that can be identified by looking at pressure measurement time histories. To illustrate this point, Fig. 7 presents both chordwise distributions of pressure coefficient mean values and samples of pressure coefficient time-history measurements from four typical orifice locations on the wing upper and lower surfaces, as shown on the airfoil schematic. The  $C_p^*$  value shown on the chordwise pressure distributions is the pressure coefficient at which the flow would reach sonic velocity on a model as determined for two-dimensional flow conditions. It is an approximate value for the three-dimensional flow conditions of this test series. However, it is a good indicator that supersonic flow

conditions exist when the pressure coefficient increases above this value. The measurements are for wing semispan station  $\eta = 0.87$  (fifth row of pressure orifices). Data are presented for the four Mach numbers that span the transonic speed range of interest. The results are for the high- $q$  test conditions for which wing-response accelerometer measurements were presented previously in Fig. 5.

At  $M = 0.80$  the chordwise distribution shows that the pressure coefficient mean values are near the  $C_p^*$  value for the forward portion of the chord. The time histories of pressure coefficient for this test condition show some flow unsteadiness at all locations but with the largest response at location 1. No coherent low-frequency content is noticeable in the pressure measurements, nor was any significant wing motion observed. At  $M = 0.88$ , the chordwise pressure distribution shows that the flow is supersonic over the forward portion of the chord. From the sample time histories of pressure coefficients, we can get an idea of just how unstable the flow is for this test condition. At location 1, which is just ahead of the strong shock on the upper surface, the flow is quite smooth. However, the situation is substantially different for locations 2, 3, and 4, where very large variations in pressure coefficients are occurring. Although the measured pressure variations at the  $M = 0.88$  test condition are large, the wing motion was considered moderate and not of sufficient magnitude to cause concern. For the  $M = 0.92$  test condition the chordwise distribution of pressure coefficient mean values indicates that a strong shock has developed on both the wing upper and lower surfaces. The flow is quite smooth at locations 1 and 3, which are ahead of the shocks, but very unsteady at locations 2 and 4, which are in the region of the shocks. The  $M = 0.92$  test condition is where the large amplitude wing motions of concern were experienced. At  $M = 0.96$  the chordwise pressure distribution indicates the flow is supersonic over the entire chord and the time histories indicate smooth flow at each of the four sample orifice locations. Wing motion at the  $M = 0.96$  test condition was insignificant.

The mean value chordwise pressure distributions of Fig. 7 also give information on when trailing-edge flow separation occurs. For this supercritical airfoil the upper surface pressure coefficient curve should cross from above to below the zero line near  $x/c = 0.95$  for attached flow conditions. Separated flow conditions are definitely indicated if the upper surface trailing-edge pressure measurement at  $x/c = 0.99$  approaches or crosses to the upper side of the zero line. Using this criteria, the mean-value pressure coefficients indicate that the upper surface trailing-edge flow is attached at  $M = 0.80$  and  $0.88$ , a slight change is observed for  $M = 0.92$ , and the flow has definitely separated at  $M = 0.96$ . For the wing lower surface, attached flow through the trailing-edge cove region of the supercritical airfoil produces the trailing-edge pressure coefficient profile shown for the  $M = 0.80$  and  $0.88$  test conditions. When the flow on the lower surface separates, the pressure coefficients for the cove region move up toward the zero line. Using this criteria, the mean-value pressure coefficients indicate that the lower surface trailing-edge flow has separated for the  $M = 0.92$  test condition. For the  $M = 0.96$  test condition the region of flow separation on the lower surface trailing edge increased further, causing the pressure coefficients to go above the zero line, as shown. Wool tufts mounted on the wing surfaces<sup>6</sup> were used to give a visual confirmation of when flow separation occurred.

### Chordwise Pressure Distributions

From the data of Fig. 7 it is obvious that it is useful to look at both the mean value of the pressure coefficients and to have an idea of the magnitude of the pressure variation that is occurring at each measurement location. Chordwise pressure distributions showing the pressure coefficient measurement range at each orifice location, as well as the mean values, are presented in Fig. 8 for spanwise station  $\eta = 0.87$  for the same four high- $q$  test conditions shown previously in Fig. 5 and 7.

The pressure coefficient measurement range is shown in the form of a vertical bar that goes from the maximum to the minimum value measured at each orifice location. The mean values and the range between minimum and maximum values were determined for a 4-s time interval for each test condition. Range was selected as the method to show the pressure variations because of the nonperiodic form of the measurements at several locations. The upper surface and lower surface pressure measurements are shown separately in order to prevent overlapping of data.

The data presented in Fig. 8 show that even at  $M = 0.80$  there is a large region of unsteady flow on the wing upper surface ( $x/c = 0.29$ – $0.58$ ). Because  $M = 0.80$  was the design cruise Mach number for the flight wing this region of flow unsteadiness was not expected, although it did not seem to cause any significant wing response motion, as was discussed earlier. At  $M = 0.88$  the upper surface measurement ranges are largest at and near the shock location. For the wing lower surface the range of measured pressure variations is quite large in the mid-chord region ( $x/c = 0.30$ – $0.51$ ), which may represent shock movement over a large chord length. Both the trailing-edge pressure coefficient measurements and the wool tufts indicated that the flow remained attached in the outboard region of the wing for this test condition. Although the pressure measurement ranges are very large at  $M = 0.88$ , the wing experienced only moderate response motion at this test condition, as was mentioned earlier.

The pressure distributions of Fig. 8 for  $M = 0.92$  show a large region of stable supersonic flow followed by a strong shock on both the wing upper and lower surfaces. The largest measurement ranges occur at the shock locations, with smaller but still significant measurement ranges occurring in the trailing-edge region behind the shocks, particularly for the wing lower surface. The pressure measurement range at the wing upper surface trailing-edge location indicates that the flow is alternating between attached and detached flow conditions. On the lower surface, from  $x/c = 0.68$  to the trailing edge, the ranges for the pressure measurements indicate that there is alternating separated and attached flow throughout the lower surface cove region. The wool tufts<sup>6</sup> indicated separated flow from  $x/c = 0.7$ – $1.0$  on the wing upper surface and from  $0.6$ – $1.0$  on the lower surface for the entire outboard wing region. The  $M = 0.92$  test condition is where the largest amplitude wing response motions occurred. At  $M = 0.96$ , where wing motion is very small, the flow is supersonic over the entire chord on both the wing upper and lower surfaces. Even so, there still seems to be a strong shock at  $x/c = 0.74$  on the upper surface and between  $x/c = 0.74$  and  $0.83$  on the lower surface. The only large measurement range observed occurs on the wing upper surface at the strong shock location. The wool tufts<sup>6</sup> indicated separated flow from  $x/c = 0.6$ – $1.0$  for both the upper and lower surfaces.

The chordwise pressure distribution presentation format of Fig. 8 does provide a good understanding of the overall flow condition at the wing station and an idea of the location and magnitude of local pressure variations. However, it does not provide information on frequency content, phasing, or coherency of any of the pressure oscillations that are occurring. A better understanding of the oscillatory characteristics of each measurement can be obtained by looking directly at the surface pressure measurement time histories. Samples of such time histories are presented in Ref. 9 for Mach numbers  $0.88$  and  $0.92$  for the outboard three orifice rows.

### $C_p$ Variations with Test Dynamic Pressure

The effects of changes in test dynamic pressure on the chordwise distribution of pressure coefficient mean values are presented in Fig. 9 for spanwise station  $\eta = 0.87$  for Mach numbers  $0.85$  and  $0.92$ . The pressure coefficient mean value is the calculated average of the measurements at each orifice location for a 4-s data interval. The Mach number selected for presentation of data prior to maximum wing response was

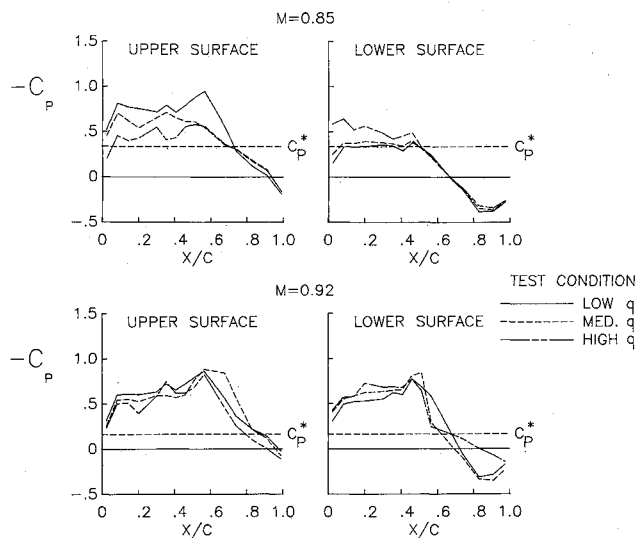


Fig. 9 Pressure distribution variations with test dynamic pressure ( $\eta = 0.87$ ).

changed from  $M = 0.88$  to  $0.85$  because data was not available for the low- $q$  test condition at  $M = 0.88$ .

At  $M = 0.85$  the mean-value pressure coefficients for the forward portion of the chord indicate that the airfoil section is effectively twisting downward to a more negative angle of attack as the dynamic pressure is increased. This is consistent with washout because of bending for an aft swept wing subjected to increased loading. At  $M = 0.92$ , the largest differences in mean-value pressure coefficient chordwise distributions for the upper surface are at the strong shock location and in the trailing-edge region. The data do not show a consistent trend, since the upper surface shock is farthest aft for the medium- $q$  test condition. On the lower surface, at  $M = 0.92$ , the small changes in mean-value pressure coefficients for the forward portion of the chord are consistent with decreasing local angle of attack with increasing test dynamic pressure. More significant differences occur on the aft portion of the chordline, where the negative pressure gradient is much steeper for the two higher  $q$  test conditions. At the high- $q$  test condition, the upward movement of the pressure coefficients in the trailing-edge region indicate that significant flow separation has occurred.

#### $C_p$ Variations with Angle of Attack

The effects of changes in angle of attack on the chordwise distribution of pressure coefficient mean values are presented in Fig. 10 for spanwise station  $\eta = 0.87$  for the medium- $q$  test condition for Mach numbers  $0.85$  and  $0.92$ . For both Mach numbers the mean-value pressure coefficients on the forward portion of the chord increase with angle of attack on the upper surface and decrease with angle of attack on the lower surface as would be expected.

At  $M = 0.85$  the mean-value pressure distributions show the existence of a strong shock on the upper surface for the two higher angles of attack. Also at  $M = 0.85$  the mean-value pressure coefficients on the aft portion of the chord are essentially independent of angle of attack, as is normal for the supercritical airfoil shape. However, at  $M = 0.92$  there are some angle of attack effects on the wing lower surface mean-value pressure distribution at the aft portion of the chord for the two most negative angles. It is believed that the changes result from more extensive flow separation at the lower surface trailing-edge region for the more negative angles of attack.

#### Concluding Remarks

The high-aspect-ratio flexible supercritical wing was tested in the NASA Langley Transonic Dynamics Tunnel to investi-

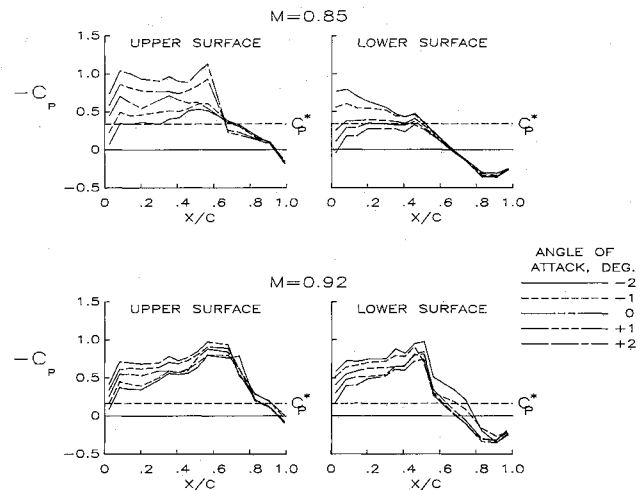


Fig. 10 Pressure distribution variations with angle of attack (medium- $q$  test condition,  $\eta = 0.87$ ).

gate a region of large wing response that occurred in the transonic speed range. Accelerometer measurements indicated that significant wing-tip motions occurred between test Mach numbers of  $0.90$  and  $0.94$  with the peak response occurring at about  $M = 0.92$ . Variation of test dynamic pressure revealed that the Mach number region of high response remained the same and that the magnitude of wing-tip motion increased as the test dynamic pressure was increased. At the peak-response test condition, the wing motion was of sufficient magnitude to cause concern for the structural safety of the wing.

Continuous wing surface-pressure time-history measurements were obtained as part of an effort to define the unsteady flow conditions forcing the response motion. The time-history measurements revealed that some unsteady flow existed even at the wing design cruise Mach number of  $0.80$  although no significant wing motion occurred. As the Mach number was increased to  $0.88$ , the wing upper surface developed steady supersonic flow over the forward chord followed by a strong shock whose location oscillated back and forth across at least one orifice location. Pressure measurements on the wing lower surface at  $M = 0.88$  revealed large variations at several mid-chord measurement locations at each span station. Although the measured pressure variations were very large at  $M = 0.88$ , the wing experienced only moderate response motion at this test condition. As the Mach number was increased to  $0.92$ , the wing developed supersonic flow over the forward portion of the chord followed by strong shocks on both the wing upper and lower surfaces. The largest amplitude pressure variations occurred at the strong shock locations, with smaller variations primarily aft of the shock in the trailing-edge region where flow separation was occurring, particularly on the wing lower surface. As stated previously, the wing motion at this test condition was of sufficient magnitude to cause concern for wing structural safety: When the test Mach number was increased to  $M = 0.96$ , the pressure measurements exhibited very small dynamic variations and the wing motion essentially disappeared.

Steady and unsteady flow conditions have been defined for the test conditions where maximum wing dynamic response occurred. The forcing function appears to be the oscillatory chordwise movement of strong shocks located on both the wing upper and lower surfaces in conjunction with the flow separating and reattaching in the trailing-edge region.

#### References

- Murrow, H. N. and Eckstrom, C. V., "Drones for Aerodynamic and Structural Testing (DAST) — A Status Report," *Journal of Aircraft*, Vol. 16, Aug. 1979, pp. 521-526.
- Sandford, M. C., Ricketts, R. H., and Hess, R. W., "Recent Transonic Unsteady Pressure Measurements at the NASA Langley Research Center," NASA TM-86408, April 1985.

<sup>3</sup>Byrdson, T. A. and Brooks, C. W., Jr., "Wind-Tunnel Investigation of Longitudinal and Lateral-Directional Stability and Control Characteristics of a 0.237-Scale Model of a Remotely Piloted Research Vehicle With a Thick, High-Aspect-Ratio Supercritical Wing," NASA TM-81790, July 1980.

<sup>4</sup>Byrdson, T. A. and Brooks, C. W., Jr., "Wind-Tunnel Investigation of Aerodynamic Loading on a 0.237-Scale Model of a Remotely Piloted Vehicle With a Thick, High-Aspect-Ratio Supercritical Wing," NASA TM-84614, June 1983.

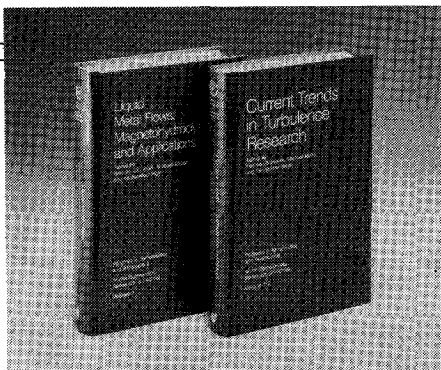
<sup>5</sup>Seidel, D. A., Sandford, M. C., and Eckstrom, C. V., "Measured Unsteady Transonic Aerodynamic Characteristics of an Elastic Supercritical Wing," *Journal of Aircraft*, Vol. 24, April 1987, p. 225.

<sup>6</sup>Seidel, D. A., Eckstrom, C. V., and Sandford, M. C., "Transonic Region of High Dynamic Response Encountered on an Elastic Supercritical Wing," *Journal of Aircraft*, Vol. 26, Sept. 1989, pp. 870-875.

<sup>7</sup>Chapin, W. G., "Dynamic-Pressure Measurements Using an Electronically Scanned Pressure Module," NASA TM-84650, July 1983.

<sup>8</sup>Eckstrom, C. V., "Loads Calibration of Strain Gage Bridges on the DAST Project Aeroelastic Research Wing (ARW-2)," NASA TM-87677, March 1986.

<sup>9</sup>Eckstrom, C. V., Seidel, D. A., and Sandford, M. C., "Unsteady Pressure and Structural Response Measurements on an Elastic Supercritical Wing," *Proceedings of the AIAA/ASME/ASCE/AHS 29th Structures, Structural Dynamics and Materials Conference*, AIAA, Washington, DC, April 1988.



## Liquid Metal Flows: Magnetohydrodynamics and Applications and Current Trends in Turbulence Research

Herman Branover, Michael Mond,  
and Yeshajahu Unger, editors

*Liquid Metal Flows: Magnetohydrodynamics and Applications (V-111)* presents worldwide trends in contemporary liquid-metal MHD research. It provides testimony to the substantial progress achieved in both the theory of MHD flows and practical applications of liquid-metal magnetohydrodynamics. It documents research on MHD flow phenomena, metallurgical applications, and MHD power generation. *Current Trends in Turbulence Research (V-112)* covers modern trends in both experimental and theoretical turbulence research. It gives a concise and comprehensive picture of the present status and results of this research.

To Order, Write, Phone, or FAX:

**AIAA** Order Department

American Institute of Aeronautics and Astronautics  
370 L'Enfant Promenade, S.W. ■ Washington, DC 20024-2518  
Phone: (202) 646-7444 ■ FAX: (202) 646-7508

V-111 1988 626 pp. Hardback  
ISBN 0-930403-43-6  
AIAA Members \$49.95  
Nonmembers \$79.95

V-112 1988 467 pp. Hardback  
ISBN 0-930403-44-4  
AIAA Members \$44.95  
Nonmembers \$72.95

Postage and handling \$4.50. Sales tax: CA residents add 7%, DC residents add 6%. Orders under \$50 must be prepaid. Foreign orders must be prepaid. Please allow 4-6 weeks for delivery. Prices are subject to change without notice.